Preparation of Ti₃C₂-PANI Composite as Sensor for Electrochemical Determination of Mercury Ions in Water

Haoliang Cheng[1,2], Jurui Yang[3,]*

[1] Faculty of Civil Engineering and Mechanics, Kunming University of Science and Technology, Kunming, Yunnan, 650500, P.R. China
[2] School of Civil Engineering, Southwest Forestry University, Kunming, Yunnan, 650224, P.R. China
[3] Faculty of Modern Agricultural Engineering, Kunming University of Science and Technology, Kunming, Yunnan, 650500, P.R. China
[*]E-mail: yangjurui@163.com

Mercury ion (Hg^{2+}) pollution is very harmful to the environment and human body. A PANI modification was applied to the surface of Ti_3C_2 slices by a simple and safe, low temperature stirring method. In this paper, a PANI-Ti_3C_2 composite with improved electrochemical performance was successfully prepared. Further study and analysis based on electrochemical tests concluded that the PANI-Ti_3C_2 composite significantly increased the electrochemical properties. The prepared composite was used as a surface modification for a glassy carbon electrode. Then, the modified electrode was used for the electrochemical determination of mercury ions. After optimization, the proposed electrochemical sensor showed a linear detection range between 0.1 and 20 μg/L with a low limit of detection of 0.017 μg/L. In addition, the proposed electrochemical sensor was successfully used for detecting mercury ions in tap water and water from Fuxian Lake.

Keywords: Electrochemical sensor; Mercury ions; Fuxian Lake; Mxene; PANI

1. INTRODUCTION

With the increasing development of society, people have begun to pay more and more attention to environmental problems. Among all kinds of pollution, heavy metal pollution is especially serious [1,2]. People are also committed to the detection and treatment of environmental pollution, and various detection methods have emerged. Heavy metals do great harm to the human body [3–5] and affect metabolism when they enter the body. Some metal ions can affect the permeability of cells so that nutrients cannot enter the cell, thereby affecting the normal function of the human body. Some metal ions can cause many diseases in the nervous system, immune system and other organs. The term "heavy

metals" generally refer to metals with a density greater than 5 g/cm^3. Common heavy metals are copper, lead, cadmium, chromium, mercury, zinc, and arsenic. These kinds of metal ions will have a great impact if present in excess in the human body [6–8].

Mercury is listed as a primary environmental pollutant monitored by the WHO. Very small amounts of mercury and its compounds can be very harmful to the human body and to the environment [9–11]. Mercury poisoning caused Minamata disease in Japan in the 1950s. Mercury accumulates when it enters the body because it is difficult to metabolize. Excess amounts can affect the nervous system, immune system and other organs, causing many diseases [12–14]. To protect human health and the environment, countries have set strict standards for mercury content in drinking water and irrigation water. In China, the standard for mercury in drinking water and irrigation water is 0.001 mg/L. It is very important to detect mercury content quickly and effectively. At present, the effective methods for detecting mercury ions include liquid chromatography, ELISA and electrochemical luminescence immunoassays, colorimetry, atomic emission spectroscopy, and electrochemical sensing [15–22].

Among them, electrochemical sensors show excellent performance towards mercury ion detection. The electrode is the key to the fabrication of an electrochemical sensor [23–30]. The type of electrodes, the properties of the modified materials and the combination of the modified materials and electrodes have important influences on the application of electrochemical sensors [31–35]. Mxene material ($M_{n+1}AX_n$) is obtained by selective corrosion of layer A. $M_{n+1}AX_n$ refers to ternary layered cermet ceramics [36–40]. Because of its special layered structure and the coexistence of three chemical bonds (metallic, ionic and covalent), it combines the excellent properties of many metals and ceramics [41,42]. Among them, M is an early transition metal element, A is a main group element from group III or IV, and X is carbon or nitrogen. Ti_2AlC, Cr_2AlC, Nb_2AlC, Ti_3SiC_2 and Ti_3AlC_2 are all $M_{n+1}AX_n$ materials. Ti_3AlC_2 is one of the most studied members of the MAX family. As a ternary layered structure material, Ti_3AlC_2 has been widely studied due to its mechanical properties, oxidation resistance, abrasion resistance and corrosion resistance. Ti_3C_2 nanocrystals have a two-dimensional layered structure similar to graphene and thus similar advantages, such as good electrical conductivity, large specific surface area and very stable physical and chemical properties. Therefore, Ti_3C_2 can be applied in many fields, such as electrochemistry and biology, and in many applications, such as sensing, photocatalysis and heavy metal ion adsorption.

Polyaniline (PANI), an excellent conductive polymer, has the advantages of high conductivity, high temperature resistance, simple synthesis method, etc. Current studies have found that PANI has good performance in electrostatic shielding, as electrode materials of capacitors and in other aspects [43–47]. The synthesis methods of PANI include chemical redox reactions, electrochemical preparation, emulsion synthesis, plasma polymerization, bulk polymerization and interfacial polymerization. The main purpose of this paper is to apply modified loads to organ-shaped Ti_3C_2 in different ways, to study the modification mechanism and to test the electrochemical properties of the obtained nanocomposites. First, PANI-Ti_3C_2 is synthesized in situ by low temperature stirring. Then, the electrochemical properties of the modified electrode were tested for the detection of mercury ions.

2. EXPERIMENTAL

Aniline, Hg^{2+} solution, and ammonium persulfate were purchased from Alfa Aesar Chemical Co., Ltd.

Preparation of Ti_3C_2: Raw powder (50 g) was weighed in the following proportion TiC:Ti:Al = 3.6:1.4:1 and then placed in a Teflon ball mill. Anhydrous ethanol was then added to the ball mill tank as a ball grinding aid and zirconia (5 nm in diameter) as a grinding medium. The mass ratio of the raw material powder, anhydrous ethanol and pellets should be 1:1:3. The ball was placed in the grinding tank and the powder mixture was ground at a speed of 300 r/min for 4 h. Next, the ball mill was used to obtain an even mixture and then it was poured into a petri dish. Finally, the mixture was put into an oven and dried at 40 °C for 24 h. The dry mixture was put into a corundum crucible and sintered without pressure. After the reaction was completely finished, the sintering furnace was allowed to cool naturally to room temperature, and a Ti_3AlC_2 ceramic block was obtained by sintering without pressure. A high energy ball mill was used to completely and fully pulverize the Ti_3AlC_2 ceramic block obtained from the unpressed sintering in the previous step; finally, the desired Ti_3AlC_2 powder was successfully prepared. At room temperature, 5 g Ti_3AlC_2 powder was slowly added into 80 mL of 40 wt.% HF and left to react for 24 h under magnetic stirring at 1200 rpm. The above corrosion products were cleaned with deionized water until the supernatant pH was > 6 after centrifugation. The substrate was freeze-dried to obtain Ti_3C_2 powder.

Preparation of the PANI-Ti_3C_2 composite: First, 0.2 g Ti_3C_2 powder was dispersed into 30 mL of 1 M hydrochloric acid solution, and then ultrasonic dispersion was conducted for 1 h to obtain a uniform suspension. Second, 100 μL pure aniline (ANI) prepared by distillation was added into the suspension and dispersed by ultrasonication for 1 h. Then, 0.335 g ammonium persulfate (APS) was dissolved in 30 mL of 1 M hydrochloric acid solution and added dropwise into the above solution. Finally, the solution was placed in an ice bath and stirred at 0 °C for 6 h. After the reaction, the reaction product was washed with ultrapure water 5 times. After cleaning, the reaction product was freeze-dried to obtain the PANI-Ti_3C_2 nanocomposite.

Electrochemical sensing: The actual samples tested were water from Fuxian Lake and tap water. Water from Fuxian Lake was used after static precipitation, filtration and removal of impurities for testing. There are two kinds of stripping voltammetry, one is anode stripping voltammetry, and the other is cathode stripping voltammetry. The detection principle is that, under certain conditions, the magnitude of the dissolution peak current is linearly related to the concentration of the detected substance. For the detection of heavy metal ions, anode stripping voltammetry should be selected. The first step was a pre-electrolysis process, which was when the measured substance was under the conditions of constant potential and uniform stirring. The main purpose was to enrich trace components to the surface of the electrode. The second step was the dissolution process, which concentrated the measured substances on the electrode surface. After the negative potential to positive sweep, the oxidation reaction occurred and redissolved, and the volt-ampere curve was recorded. In a three-electrode system, Ti_3C_2/GCE or PANI-Ti_3C_2 were the working electrode, a platinum electrode was the auxiliary electrode, and a silver chloride electrode was the reference electrode. The electrochemical reaction was scanned and recorded in 10 mL of 0.005 M sulfuric acid solution using anodic stripping voltammetry (ASV). The scanning interval was

0-0.6 V, the scanning speed was 100 mV/s, the stationary time was 30 s, the enrichment time was 500 s, the enrichment potential was -0.6 V, and the working frequency was 50 Hz.

3. RESULTS AND DISCUSSION

Figure 1A shows the XRD patterns of the prepared PANI, Ti_3C_2 and PANI-Ti_3C_2. It can be seen from the figure that the XRD peak of PANI at 2 theta =20.5° corresponds to the (020) crystal surface of PANI. The diffraction peak of Ti_3C_2 on the (002) crystal plane shifts to the left along the x-axis from that of the Ti_3AlC_2 parent phase, which makes the XRD characteristic peak of Ti_3C_2 weaker and wider. Such an XRD pattern can show that the degree of crystallinity and the degree of structural order of Ti_3C_2 decreases greatly. In the XRD diagram of Ti_3C_2, the diffraction peaks at 2 theta =7.1°, 17°, 28°, 35°, 41° and 61° correspond to the crystal planes of (002), (006), (008), (0010), (0012) and (110), respectively. Compared with the XRD pattern of Ti_3C_2, the XRD pattern of PANI-Ti_3C_2 shows a new diffraction peak at 2 theta =20.7°, corresponding to the (020) crystal surface of PANI. The XRD peak of PANI-Ti_3C_2 at 2 theta =26° corresponds to TiO_2. This value is because a small amount of Ti_3C_2 is oxidized when ammonium persulfate, an oxidant, is added in the preparation of the PANI-Ti_3C_2 composite material. Therefore, the phase analysis shows the successful preparation of the PANI-Ti_3C_2 nanocomposite. Ti_3C_2 allows for easy immobilization of enzymes/protein onto its surface, thus acting as a promising support to achieve DET with accelerated electrode kinetics, low detection limits, and high sensitivity and selectivity [48].
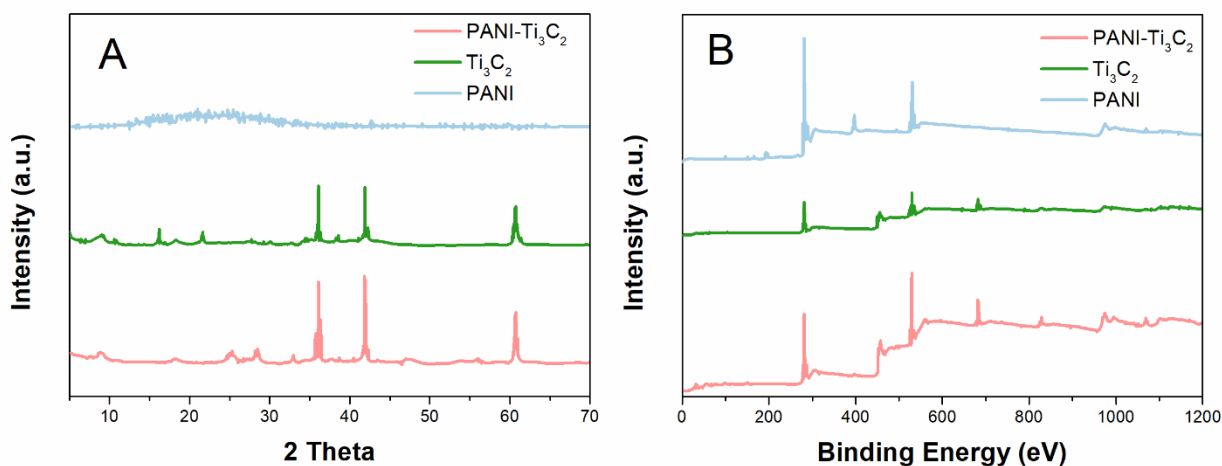

Figure 1. (A) XRD patterns of PANI, Ti_3C_2 and PANI-Ti_3C_2. (B) XPS spectras of PANI, Ti_3C_2 and PANI-Ti_3C_2.

Figure 1B shows the XPS spectra of the prepared PANI, Ti_3C_2 and PANI-Ti_3C_2. As seen from the figure, the characteristic peaks C_{1s}, O_{1s}, F_{1s} and Ti_{2p} appear, proving the existence of Ti_3C_2. At the same time, the appearance of O_{1s} and F_{1s} characteristic peaks prove the existence of -O, -OH and -F functional groups on the Ti_3C_2 laminates. The appearance of C_{1s} and N_{1s} peaks prove the successful preparation of PANI. Compared with Ti_3C_2, the XPS broad spectrum of PANI-Ti_3C_2 shows an N_{1s} peak,

which further proves the successful preparation of the PANI-Ti$_3$C$_2$ nanocomposites under the condition of low temperature stirring. The above results were consistent with the results of the XRD analysis. By integral fitting, the N$_{1s}$ analysis of the XPS spectra for the PANI-Ti$_3$C$_2$ nanocomposite showed four characteristic peaks at 397.1 eV, 398.2 eV, 400.1 eV and 400.5 eV, corresponding to the imine structure (=NH-), amino group (-NH-), N atom (N$^{\bullet}$+) with a positron and protonated amino groups, respectively. The results show that the PANI-Ti$_3$C$_2$ nanocomposite is successfully prepared by a low temperature oxidation reaction between Ti$_3$C$_2$ and aniline.
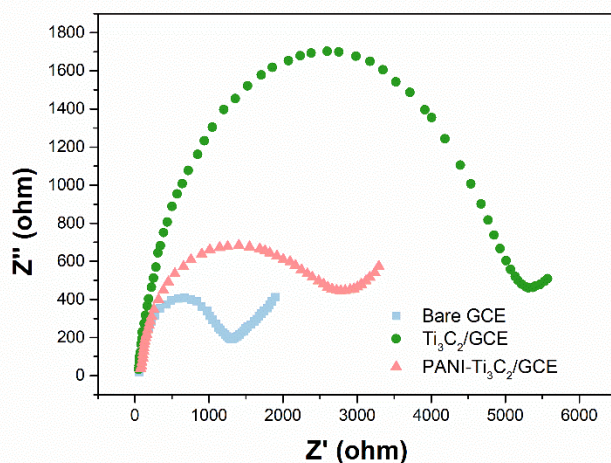

Figure 2. EIS spectra of the (a) GCE, (b) Ti$_3$C$_2$ and (c) PANI-Ti$_3$C$_2$ in in 5 mM [Fe(CN)$_6$]$^{3-/4-}$.
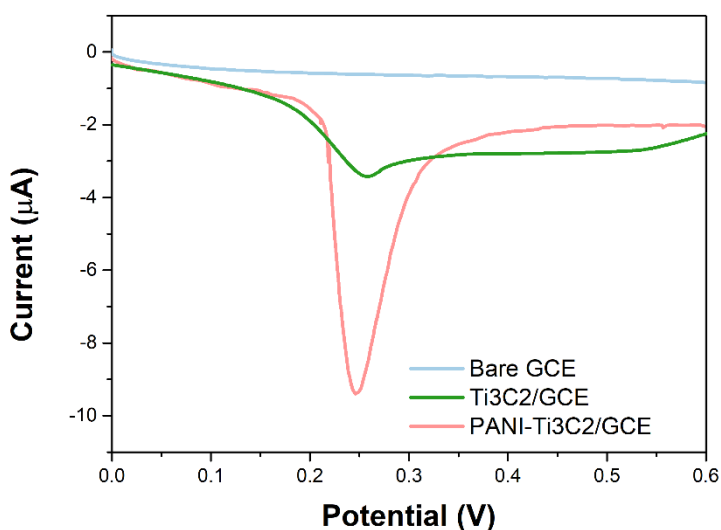
Figure 3. ASV of (a) GCE, (b) Ti$_3$C$_2$ and (c) PANI-Ti$_3$C$_2$ towards 10 µg/L mercury ion. (0.005 M H$_2$SO$_4$; scanning rate: 100 mV/s; stationary time: 30 s, accumulation time: 500 s, accumulation potential: -0.6 V, frequency:50 Hz.)

The impedance shown in Figure 2 was measured in a mixture of 0.1 M KCl and 0.1 M [Fe(CN)$_6$]$^{3-/4-}$ in a 1:1 ratio. It can be seen from the figure that the impedance of the bare electrode is relatively small, while the impedance of the modified electrode is significantly larger than that of the bare electrode,

which indicates that Ti_3C_2 has been successfully modified to the electrode surface. As seen from the comparison between curve b and curve c, the impedance of PANI-Ti_3C_2 is significantly reduced compared with that of Ti_3C_2, which means that the PANI surface modification can significantly enhance the electron transfer rate.

A bare GCE, Ti_3C_2-modified GCE and PANI-Ti_3C_2-modified GCE were successively put into 10 μg/L mercury ion solution and tested by anodic stripping voltammetry. The results are shown in Figure 3. There is almost no signal on the bare GCE, while there is a peak of approximately 0.25 V on the Ti_3C_2-modified GCE and PANI-Ti_3C_2-modified GCE, indicating that Ti_3C_2 modified on the surface of the electrode adsorbs the mercury ions well. Interestingly, the dissolution voltammetry curve of the Ti_3C_2-modified electrode is almost the same as that of the PANI-Ti_3C_2-modified electrode, but the peak value of the PANI-Ti_3C_2-modified electrode is larger and the peak shape is more regular. In fact, given the strong affinity and high diffusivity of Hg, there is a great possibility for Hg to diffuse into the interior of Ti_3C_2, which can occur when a large amount of elemental Hg is deposited at the interface of the Ti_3C_2 and electrolyte [49]. Therefore, the PANI-Ti_3C_2 modified electrode is more suitable for the detection of mercury ions.

Figure 4A shows PANI-Ti_3C_2-modified electrodes detecting responses in samples with 10 μg/L mercury ions over a pH range of 1 to 6. The figure shows that pH has a relatively large influence on the peak current. The peak current increases with increasing pH before a pH of 2, which may be due to the interference of the hydrogen ion concentration on PANI-Ti_3C_2 when the pH is too low. The increase and decrease after a pH value of 2 may be because mercury ions begin to undergo hydrolysis or change in chemical valence with the increase in pH value, thus reducing the electrochemical response. The maximum electrochemical response occurs at a pH of 2. Therefore, sulfuric acid solutions with a pH of 2 were selected for subsequent testing.

Deposition potential also has a great influence on the electrochemical performance of electrochemical sensors, so it is very important to find a suitable deposition potential. The deposition potentials of the PANI-Ti_3C_2-modified electrode were 0, -0.2, -0.4, -0.6, -0.8 and -1.0 V , and a mercury ion concentration of 10 μg/L was used for detection. As shown in Figure 4B, the maximum current occurs when the deposition potential is -0.6 V. Shifting the potential positive or negative decreases the electrochemical response, possibly because mercury ions are not sufficiently enriched when the potential is not sufficiently negative. When the potential is too negative, hydrogen evolution may occur in the solution. Therefore, the deposition potential of -0.6 V is chosen for the subsequent experiments.

The accumulation time also has a certain influence on the electrochemical response of the experiment. During the experiment, the peak current was measured when the deposition time was 100, 200, 300, 400, 500 and 600 s. As shown in Figure 4C, before 500 s, the peak current increases with increasing deposition time and then tends to level off. This phenomenon proves that at 500 s, the adsorption of mercury ions on the electrode surface reaches a saturation state. Therefore, 500 s is selected as the subsequent accumulation time.
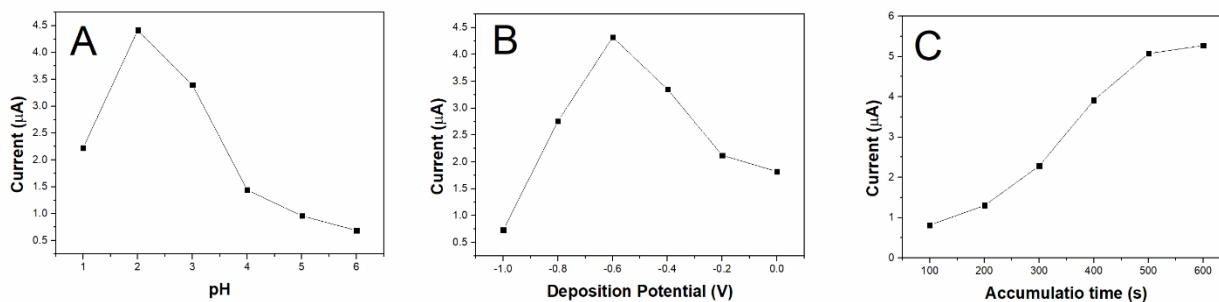
Figure 4. Effect of (A) pH condition, (B) deposition potential and (C) accumulation time in PANI-Ti$_3$C$_2$ modified electrode for 10 μg/L mercury ions detection.

The effect of PANI-Ti$_3$C$_2$ on the electrochemical response was also studied. Under the above optimal conditions, the peak currents of PANI-Ti$_3$C$_2$ with 5, 10, 15 and 20 μL were measured. As shown in Figure 5, the electrochemical response increases gradually from 5 to 10 μL. Further increases in the amount of the modifier lead to a decrease in the stripping peak current due to a high mass-transfer resistance. The reduction time is important in stripping voltammetry [50]. From 10 μL to 20 μL, the peak current gradually decreases, probably because the electrode becomes unstable as the amount of stripping increases. Thus, in subsequent experiments, the electrode is modified to 10 μL.
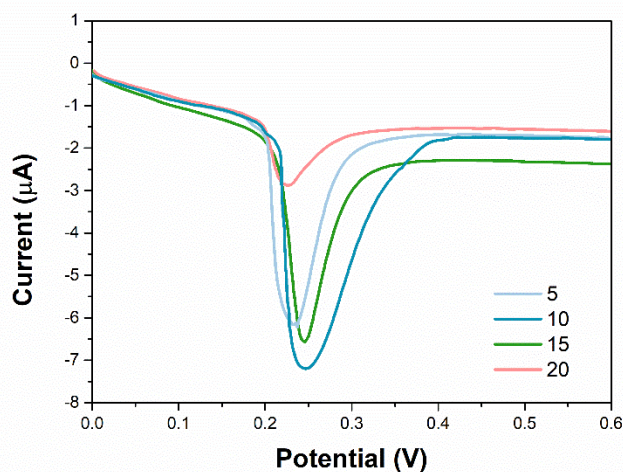

Figure 5. ASV of different amount of PANI-Ti$_3$C$_2$ modification on sensing performance. (0.005 M H$_2$SO$_4$; scanning rate: 100 mV/s; stationary time: 30 s, accumulation time: 500 s, accumulation potential: -0.6 V, frequency:50 Hz.)

Figure 6 studies the relationship between the peak current and the concentration of mercury ions. The peak current increases with an increasing concentration of mercury ions. Furthermore, the peak current increases linearly with the concentration of mercury ions in a range of 0.1-20 μg/L. The detection limit is 0.017 μg/L (S/N=3). Therefore, the PANI-Ti$_3$C$_2$-modified electrode is very good at detecting mercury ions. Table 1 shows the comparison of this work with other references. Adsorption energy calculations can provide insight into the strong stripping peak exhibited by the mercury ions adsorbed

on the PANI-Ti$_3$C$_2$. The adsorption energies of mercury ions on the (200) and (220) faces of PANI-Ti$_3$C$_2$ were -13.23 and -15.11, respectively. These values are much more negative than those for other metal ions, suggesting there is a strong interaction between the mercury ions and PANI-Ti$_3$C$_2$ [51–55].
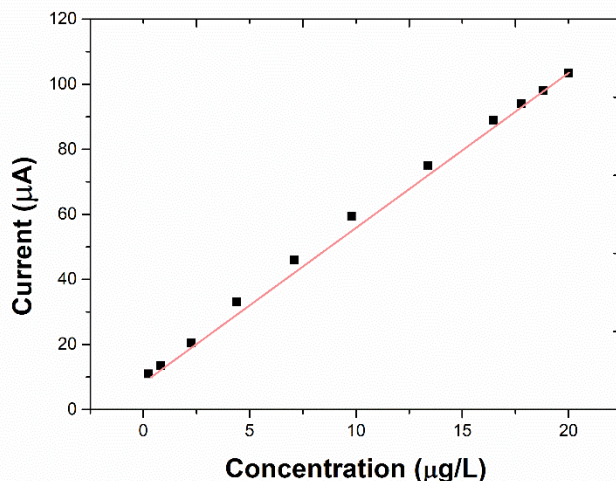

Figure 6. The relationship between peak current and the concentration of the mercury ions.

Table 1. Comparison of mercury ions detection using the proposed electrode with other electrochemical sensor.

Electrode	Linear detection range	Limit of detection	Reference
Ion imprinted polymeric nanobeads	80-200 μg/L	0.1 μg/L	[56]
Ion imprinted polymer	1-8000 μg/L	0.19 μg/L	[57]
Mercury ion imprinted polymer	2.5–500 μg/L	0.52 μg/L	[58]
g-C$_3$N$_4$ and Hg(II) -imprinted polymer nanoparticles	0.06–25 μg/L	0.018 μg/L	[56]
Microporous poly(2-mercaptobenzothiazole) films	1–160μg/L	0.1 μg/L	[59]
PANI-Ti$_3$C$_2$	0.1-20 μg/L	0.017 μg/L	This work

Selectivity is one of the most important indexes for electrochemical sensors. To investigate the selectivity of the PANI-Ti$_3$C$_2$-modified electrode, the best experimental conditions were used. The electrode first detected the electrochemical signal of a solution with a concentration of 10 μg/L mercury ions and then other metal ions with different concentrations (100 μg/L Fe^{3+}, 100 μg/L Co^{2+}, 100 μg/L Ni^{2+}, 100 μg/L Pb^{2+}, 50 μg/L Cu^{2+}, 100 μg/L Na$^+$, 100 μg/L K$^+$) were added. The PANI-Ti$_3$C$_2$-modified electrode has good selectivity and can be used for the detection of complex systems.
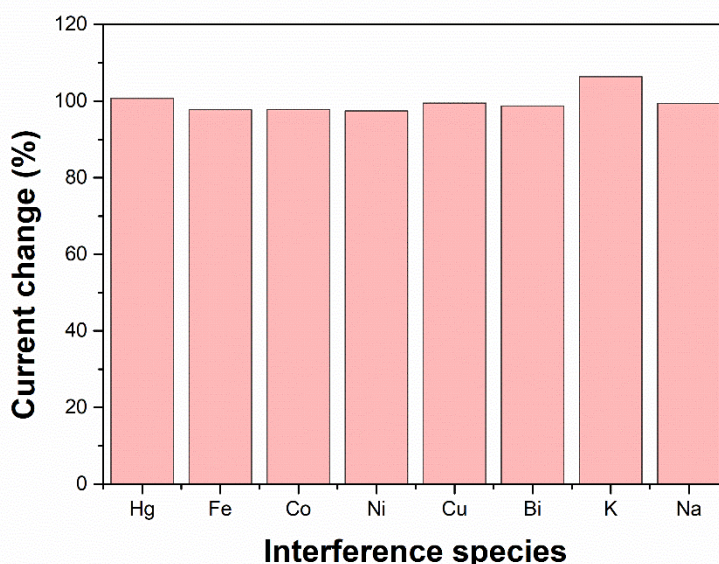
Figure 7. Selectivity performance of the PANI-Ti$_3$C$_2$ modified electrode for mercury ions sensing.

To investigate whether the PANI-Ti$_3$C$_2$-modified electrode is feasible in actual sample detection, a standard recovery method was used to detect the mercury ion content in tap water and water from Fuxian Lake; additionally, ICP-OES was used to detect and compare the above processed actual samples. As shown in Table 2, the recovery of the modified electrode is within the range of 97.2-100.8%, which is consistent with the ICP-OES test data. Thus, the PANI-Ti$_3$C$_2$-modified electrode can be used for the detection of actual samples with high accuracy.

Table 2. Determination of mercury ions in tap water and Fuxian lake using the proposed electrochemical sensor and ICP-OES.

Sample	Added (μg/L)	Detected (μg/L)	Recovery rate (%)	ICP-OES (μg/L)
Tap water	0	0	-	0
	1	0.972	97.2	1.021
	1	1.968	98.4	1.957
	2	4.031	100.8	3.977
Fuxian lake	0	0	-	0
	1	0.988	98.8	1.023
	1	1.989	99.5	2.076
	2	4.022	100.6	4.102

4. CONCLUSION

In this experiment, an electrochemical sensor formed by a PANI-Ti$_3$C$_2$-modified electrode was used to detect mercury ions. Due to the adsorption and complexation of mercury ions on PANI-Ti$_3$C$_2$, the sensor has a good electrochemical response to mercury ions. The linear range of detection is 0.1-20

µg/L, and the detection limit is 0.017 µg/L (S/N=3). The electrode has good stability and reproducibility and a good recovery rate in the detection of mercury ions in tap water and lake water.

References

1. D. Paul, *Ann. Agrar. Sci.*, 15 (2017) 278.
2. M.S. Islam, M.K. Ahmed, M. Raknuzzaman, M. Habibullah-Al-Mamun, M.K. Islam, *Ecol. Indic.*, 48 (2015) 2821.
3. W. Gao, H.Y. Nyein, Z. Shahpar, H.M. Fahad, K. Chen, S. Emaminejad, Y. Gao, L.-C. Tai, H. Ota, E. Wu, *Acs Sens.*, 1 (2016) 866.
4. P. Chen, X. Bi, J. Zhang, J. Wu, Y. Feng, *Particuology*, 20 (2015) 104.
5. X. Qing, Z. Yutong, L. Shenggao, *Ecotoxicol. Environ. Saf.*, 120 (2015) 377.
6. M. Taseidifar, F. Makavipour, R.M. Pashley, A.M. Rahman, *Environ. Technol. Innov.*, 8 (2017) 182.
7. Y. Liu, Y. Deng, H. Dong, K. Liu, N. He, *Sci. China Chem.*, 60 (2017) 329.
8. A. Abbas, A.M. Al-Amer, T. Laoui, M.J. Al-Marri, M.S. Nasser, M. Khraisheh, M.A. Atieh, *Sep. Purif. Technol.*, 157 (2016) 141.
9. S. Malar, S.V. Sahi, P.J. Favas, P. Venkatachalam, *Environ. Sci. Pollut. Res.*, 22 (2015) 4597.
10. E. García-Ordiales, J.M. Esbrí, S. Covelli, M.A. López-Berdonces, P.L. Higueras, J. Loredo, *Environ. Sci. Pollut. Res.*, 23 (2016) 6024.
11. S. Malar, S. Sahi, P. Favas, P. Venkatachalam, *Int. J. Environ. Sci. Technol.*, 12 (2015) 3273.
12. J. Marrugo-Negrete, G. Enamorado-Montes, J. Durango-Hernández, J. Pinedo-Hernández, S. Díez, *Chemosphere*, 167 (2017) 188.
13. H. Xing, J. Xu, X. Zhu, X. Duan, L. Lu, W. Wang, Y. Zhang, T. Yang, *J. Electroanal. Chem.*, 760 (2016) 52.
14. M.-P.N. Bui, J. Brockgreitens, S. Ahmed, A. Abbas, *Biosens. Bioelectron.*, 85 (2016) 280.
15. J. Zhao, M. Huang, L. Zhang, M. Zou, D. Chen, Y. Huang, S. Zhao, *Anal. Chem.*, 89 (2017) 8044.
16. X. Zhang, Z. Dai, S. Si, X. Zhang, W. Wu, H. Deng, F. Wang, X. Xiao, C. Jiang, *Small*, 13 (2017) 1603347.
17. H. Huang, Y. Weng, L. Zheng, B. Yao, W. Weng, X. Lin, *J. Colloid Interface Sci.*, 506 (2017) 373.
18. N.T.N. Anh, A.D. Chowdhury, R. Doong, *Sens. Actuators B Chem.*, 252 (2017) 1169.
19. Y.-W. Wang, L. Wang, F. An, H. Xu, Z. Yin, S. Tang, H.-H. Yang, H. Song, *Anal. Chim. Acta*, 980 (2017) 72.
20. G. Yang, H. Zhang, Y. Wang, X. Liu, Z. Luo, J. Yao, *Sens. Actuators B Chem.*, 251 (2017) 773.
21. Y. Liu, Y. Deng, T. Li, Z. Chen, H. Chen, S. Li, H. Liu, *J. Biomed. Nanotechnol.*, 14 (2018) 2156.
22. L.-L. He, L. Cheng, Y. Lin, H.-F. Cui, N. Hong, H. Peng, D.-R. Kong, C.-D. Chen, J. Zhang, G.-B. Wei, *J. Electroanal. Chem.*, 814 (2018) 161.
23. M. Hong, M. Wang, J. Wang, X. Xu, Z. Lin, *Biosens. Bioelectron.*, 94 (2017) 19.
24. N. Wang, G. Liu, H. Dai, H. Ma, M. Lin, *Anal. Chim. Acta*, 1062 (2019) 140.
25. H.L. Nguyen, H.H. Cao, D.T. Nguyen, V. Nguyen, *Electroanalysis*, 29 (2017) 595.
26. N.R. Devi, M. Sasidharan, A.K. Sundramoorthy, *J. Electrochem. Soc.*, 165 (2018) B3046.
27. M.A. Deshmukh, R. Celiesiute, A. Ramanaviciene, M.D. Shirsat, A. Ramanavicius, *Electrochimica Acta*, 259 (2018) 930.

28. M. R Ganjali, T. Alizadeh, B. Larijani, M. Aghazadeh, E. Pourbasheer, P. Norouzi, *Curr. Anal. Chem.*, 13 (2017) 62.
29. Y. Zhang, C. Zhang, R. Ma, X. Du, W. Dong, Y. Chen, Q. Chen, *Mater. Sci. Eng. C*, 75 (2017) 175.
30. L. Tang, X. Xie, Y. Zhou, G. Zeng, J. Tang, Y. Wu, B. Long, B. Peng, J. Zhu, *Biochem. Eng. J.*, 117 (2017) 7.
31. L. Fu, A. Wang, G. Lai, C.-T. Lin, J. Yu, A. Yu, Z. Liu, K. Xie, W. Su, *Microchim. Acta*, 185 (2018) 87.
32. L. Fu, A. Wang, G. Lai, W. Su, F. Malherbe, J. Yu, C.-T. Lin, A. Yu, *Talanta*, 180 (2018) 248.
33. L. Fu, Y. Xu, J. Du, D. Cao, Q. Liu, *Int. J. Electrochem. Sci.*, 14 (2019) 4383.
34. L. Fu, A. Wang, F. Lyv, G. Lai, H. Zhang, J. Yu, C.-T. Lin, A. Yu, W. Su, *Bioelectrochemistry*, 121 (2018) 7.
35. L. Fu, Y. Zheng, P. Zhang, J. Zhu, H. Zhang, L. Zhang, W. Su, *Electrochem. Commun.*, 92 (2018) 39.
36. X. Liang, Y. Rangom, C.Y. Kwok, Q. Pang, L.F. Nazar, *Adv. Mater.*, 29 (2017) 1603040.
37. M. Zhao, X. Xie, C.E. Ren, T. Makaryan, B. Anasori, G. Wang, Y. Gogotsi, *Adv. Mater.*, 29 (2017) 1702410.
38. J. Yan, C.E. Ren, K. Maleski, C.B. Hatter, B. Anasori, P. Urbankowski, A. Sarycheva, Y. Gogotsi, *Adv. Funct. Mater.*, 27 (2017) 1701264.
39. Q. Jiang, N. Kurra, M. Alhabeb, Y. Gogotsi, H.N. Alshareef, *Adv. Energy Mater.*, 8 (2018) 1703043.
40. L. Ding, Y. Wei, Y. Wang, H. Chen, J. Caro, H. Wang, *Angew. Chem. Int. Ed.*, 56 (2017) 1825–1829.
41. L. Fu, K. Xie, Y. Zheng, L. Zhang, W. Su, *Electronics*, 7 (2018) 15.
42. L. Fu, Z. Liu, Y. Huang, G. Lai, H. Zhang, W. Su, J. Yu, A. Wang, C.-T. Lin, A. Yu, *J. Electroanal. Chem.*, 817 (2018) 128.
43. A. Ladrón-de-Guevara, A. Boscá, J. Pedrós, E. Climent-Pascual, A. De Andrés, F. Calle, J. Martínez, *Appl. Surf. Sci.*, 467 (2019) 691.
44. N. Hui, X. Sun, S. Niu, X. Luo, *ACS Appl. Mater. Interfaces*, 9 (2017) 2914.
45. Y. Qu, C. Lu, Y. Su, D. Cui, Y. He, C. Zhang, M. Cai, F. Zhang, X. Feng, X. Zhuang, *Carbon*, 127 (2018) 77.
46. Y. Navale, S. Navale, M. Chougule, S. Ingole, F. Stadler, R.S. Mane, M. Naushad, V. Patil, *J. Colloid Interface Sci.*, 487 (2017) 458.
47. J. Deng, T. Wang, J. Guo, P. Liu, *Prog. Nat. Sci. Mater. Int.*, 27 (2017) 257.
48. A. Sinha, Dhanjai, H. Zhao, Y. Huang, X. Lu, J. Chen, R. Jain, *TrAC Trends Anal. Chem.*, 105 (2018) 424.
49. Y. Liu, C.Z. Huang, *ACS Nano*, 7 (2013) 11026.
50. L. Fu, K. Xie, A. Wang, F. Lyu, J. Ge, L. Zhang, H. Zhang, W. Su, Y.-L. Hou, C. Zhou, C. Wang, S. Ruan, *Anal. Chim. Acta*, 1081 (2019) 51.
51. R. Mo, Q. Yuan, X. Yan, T. Su, Y. Feng, L. Lv, C. Zhou, P. Hong, S. Sun, C. Li, *J. Electrochem. Soc.*, 165 (2018) H750.
52. Y. Liu, Y. Deng, T. Li, Z. Chen, H. Chen, S. Li, H. Liu, *J. Biomed. Nanotechnol.*, 14 (2018) 2156.
53. A.M. Ashrafi, Z. Koudelkova, E. Sedlackova, L. Richtera, V. Adam, *J. Electrochem. Soc.*, 165 (2018) B824.
54. N.R. Devi, M. Sasidharan, A.K. Sundramoorthy, *J. Electrochem. Soc.*, 165 (2018) B3046.
55. N. Wang, G. Liu, H. Dai, H. Ma, M. Lin, *Anal. Chim. Acta*, 1062 (2019) 140.
56. M.R. Ganjali, A.R. Rahmani, R. Shokoohi, A. Farmany, M. Khazaei, *Int J Electrochem Sci*, 14 (2019) 6420.
57. A. Afkhami, T. Madrakian, M. Soltani-Shahrivar, M. Ahmadi, H. Ghaedi, *J. Electrochem. Soc.*, 163 (2016) B68.

58. T. Alizadeh, M.R. Ganjali, M. Zare, *Anal. Chim. Acta*, 689 (2011) 52.
59. X.-C. Fu, X. Chen, Z. Guo, C.-G. Xie, L.-T. Kong, J.-H. Liu, X.-J. Huang, *Anal. Chim. Acta*, 685 (2011) 21.